Supplementary Information for:

# *OPA1* disease-causing mutants have domain-specific effects on mitochondrial ultrastructure and fusion

Benjamín Cartes-Saavedra[a,b,1], Daniel Lagos[a,1], Josefa Macuada[a], Duxan Arancibia[a,c], Florence Burté[d] , Marcela K. Sjöberg-Herrera[a], María Estela Andrés[a], Rita Horvath[e], Patrick Yu-Wai-Man[e,f,g,h,i], György Hajnóczky[b], and Verónica Eisner[a,2], ✉ veisner@bio.puc.cl

[1]These authors contributed equally to this work

## SI Materials and Methods

### Cell culture

All cells were cultured in high glucose Dulbecco-Eagle modified medium conatining sodyum pyruvate (DMEM, Gibco Cat#1280017) and supplemented with 10% of fetal bovine serum (FBS), 2mM glutamine, and 100 U/ml penicillin and 100 μg/mL streptomycin in humidified air (5% CO2) at 37ºC, unless stated otherwise. Skeletal muscle-derived fibroblasts were generated from myoblast samples. The patient's derived myoblasts were cultured in Skeletal Muscle Cell Growth Medium (PromoCell #CatC-23160) and plated in collagen I-coated dishes. Cells were trypsinized and preplated in an uncoated dish for 30 mins to separate fibroblasts from myoblasts, where the first adhere to the uncoated dish while the second were resuspended and plated in collagen I-coated dishes. The patient's fibroblasts were used between passages 3-9. All the cells were tested for mycoplasma contamination regularly using the following protocol (1). The cells were cultured following the institutional ethic protocols.

### Western blot analysis

Cells were cultured to 70-80% of confluence, harvested and frozen. After thawing, a membrane-rich lysate was generated by RIPA buffer supplemented with protease and phosphatase inhibitors; 30 μg of total protein extracts were loaded into 8% SDS-PAGE gel and transferred to PVDF membranes. Membranes were blocked with 5% milk in 0.1% TBS-Tween for 1 hour at RT followed by an overnight incubation with primary antibody prepared in 5%milk or 3%BSA in 0.1% TBS-Tween (For antibodies, see **Table 1**). Commercial antibodies for OPA1 recognize epitopes located that the "dynamin" domain, that is, in between the GTPase and the GED domains. The following secondary antibodies were prepared with 5% milk in 0.1% TBS-Tween. The specificity of Opa1, Mfn1, and Mfn2 antibodies was verified in *Opa1*$^{-/-}$, *Mfn1*$^{-/-}$, and *Mfn2*$^{-/-}$ MEFs, respectively, where Western Blot bands of each protein were undetected. Secondary antibodies were visualized with enhanced chemiluminescent substrates (ECL, SuperSignal West Dura or SuperSignal West Femto, Thermo Scientific). Densitometry was performed using ImageStudio software (LI-COR Bioscience).

**Table 1. Antibodies used for Western blot analysis.**

| Epitope | Dilution | Source |
|---|---|---|
| OPA1 | 1:1000 | BD Transduction Laboratories Cat #612607 |
| MFN2 | 1:1000 | Abcam Cat #ab50838 |
| MIC60 | 1:1000 | Proteintech Cat #10179-1-AP |
| MIC19 | 1:1000 | Proteintech Cat #256225-1-AP |
| MFN1 | 1:1000 | Abcam Cat #126575 |
| DRP1 | 1:1000 | BD Transduction Laboratories Cat #611113 |
| pDRP1-ser616 | 1:1000 | Cell Signaling Cat #3455 |
| mtHsp70 | 1:1000 | Thermo Fisher Cat #MA3-028 |
| TOMM20 | 1:1000 | Cell Signaling Cat #42406 |
| GAPDH | 1:5000 | Proteintech Cat #60004-1-lg |
| Tubulin | 1:2000 | Abcam Cat #Ab6160 |
| Rabbit IgG HRP | 1:5000 | Jackson ImmunoResearch, Cat #111-035-045 |
| Mouse IgG HRP | 1:5000 | Jackson ImmunoResearch Cat #115-035-062 |
| Rat IgG HRP | 1:5000 | Proteintech Cat #SA00001-15 |

**Cell transfection**

Cells were plated on 1.5 mm glass coverslips and then each plate was transfected with 1 μg of DNA of the construct of interest. Plasmid delivery was performed using OPTI-mem (Thermofisher) or Transfectagro (Corning) and Lipofectamine 2000 or 3000 according to the manufacturer's protocol. For optimal expression, the cells were grown 24-48h after transfection.

**Transmission electron microscopy (TEM)**

To evaluate ultrastructure and cristae content, pellets of $8x10^5$ cells were fixed with glutaraldehyde 2.5%. Staining was performed as previously described (2) Images of ultra-thin sections were acquired in a transmission electron microscope Philips Tecnai 12 at 80 kV, at the Advanced Microscopy Facility, Pontificia Universidad Católica de Chile. Analysis

of area, shape and cristae dimensions was performed with Fiji Image J. **Mitochondrial shape**: Bullet and worm shape descriptors are based on the roundness index. Mitochondria with a roundness index higher than 0.5 were classified as bullet-like, and mitochondrial with an index lower than 0.5 were classified as worm-like. Aberrant organelles comprise the elongated mitochondria with partial swelling and interruptions in the cristae abundance, as well as the balloon-like, swollen mitochondria. **Mitochondria cristae shape:** A Semi-quantitative analysis was used for classification. Mitochondria without cristae were classified as empty mitochondria. Mitochondria with short cristae with or without a junction were classified as short when less than 50% of the cristae protruded into the mitochondrial matrix. Mitochondria with long, well-defined cristae with or without a junction were classified as long cristae when at least 50% of the cristae protruded into the mitochondrial matrix. **Cristae Junction width** was determined as the minimal distance between the 2 sides of the IMM in the proximity of the curvature that forms the cristae. **Cristae Lumen width** was measured as the maximal distance between the IMM in the proximity of the bottom of the cristae.

**RNA isolation and cDNA synthesis**

Control, *OPA1* c.870+5G>A and *OPA1* c.2818+5G>A patient's cells were grown in a 100 mm dish until confluent. Next, cells were washed twice with PBS, frozen with liquid nitrogen, and stored at -80ºC. RNA isolation was performed using TRIzol (Invitrogen) according to manufacturer protocol and stored at -80ºC. cDNA preparation was done by using the AffinityScript cDNA Synthesis Kit (Agilent Technologies) according to the manufacturer's protocol. 1 ug of RNA was used as a template and oligo-dT primers were used in each retro transcription reaction. Next, cDNA products were amplified by RT-PCR using primers designed to amplify exons 7-9 or 25-58. PCR products were separated by 2% agarose gel (Ultrapure Low Melting Point Agarose, Invitrogen) to determine the heterozygous splicing defect. Given that the effect of *OPA1* c.2818+5G>A mutant over exon 27 had not been described, wild-type and mutant PCR amplicons were purified using the PureLink Quick Gel Extraction Kit (Invitrogen) according to the manufacturer's protocol and sequenced to confirm the skipping of exon 27. OPA1 wild-type allele from the *OPA1* c.2818+5G>A and Control patient's cells were sequenced as a control and used as a template for Blast analysis. For primers details, see **Table 2.**

**Table 2. Primers used to amplify Exon 8 and Exon 27 from OPA1 isoform 1 (*Homo sapiens*)**

| Exon | Sequence (5'-3') |
|---|---|
| **OPA1 Exon 8 forward** | TGCAGAAAGATGACAAAGGCA |
| **OPA1 Exon 8 reverse** | TGGGCAATCATTTCCAACACAC |
| **OPA1 Exon 27 forward** | TGATGTGGTCTTGTTTTGGCG |
| **OPA1 Exon 27 reverse** | TGCAGAGCTGATTATGAGTACGA |

***In silico* OPA1 splicing predictions of *OPA1* mutants**

Both *OPA1* c.870+5G>A and *OPA1* c.2818+5G>A exhibited intronic point mutations 5 bp downstream the exons 8 or 27, respectively. To understand the mechanism behind the splicing defect, the sequences containing the intronic mutation *OPA1* c.870+5G>A and *OPA1* c.2818+5G>A were analyzed by two online algorithms: Human Splice Finder (HSF) score and Maximum Entropy Score (MaxEnt) (3, 4). *Homo sapiens* OPA1 transcript variant 1 was used as a template (NM_015560.2).

**OPA1 domain-specific mutations plasmid construction**

pCCEY plasmid containing human OPA1 isoform 1 WT was kindly donated by Guy Lenaers. Mutagenic OPA1 variants were designed using the Q5 Site-Directed Mutagenesis Kit (New England Biolabs), following the manufacturer's protocol. The generation of the specific mutations was confirmed through sequencing using the ABI PRISM 3500 xl Applied Biosystems (FONDEQUIP EQM150077) at Pontificia Universidad Católica de Chile or sequenced at Macrogene inc, Seoul, South Korea. pCCEY plasmid encoding GTPase mutant *OPA1* c.899G>A (G300E) and GED mutant *OPA1* c.2708delTTAG was kindly donated by Guy Lenaers and used in previous studies (5, 6). For primer details, see **Table 3**.

**Table 3. Primers used to build the mutants generated in this work.**

| Mutant | Primers |
|---|---|
| *OPA1* c.870+5G>A | 5' GTTGTTGTGGTTGGAGATC 3' |
| | 3' CTTAAGCTTTCTATGATGAATG 5' |
| *OPA1* c.889C>T | 5' GGTTGGAGATtAGAGTGCTGG 3' |
| | 3' ACAACAACCCGTGGCAGA 5' |

| | |
|---|---|
| *OPA1* c.1334G>A | 5’ GATGCTGAACaCAGTATTGTTAC 3’ |
| | 3’ CACAGATCCATCTTGAATAC 5’ |
| *OPA1* c.2713C>T | 5' TGAAGTTAGGtGATTAGAGAAAAATG 3' |
| | 3' GTATTTGTAAGTTGTTGCC 5' |
| *OPA1* c.2818+5G>A | 5' AGAAAGTTAGAGAAATTCAAGAAAAAC 3' |
| | 3' CTTCAGTATTTGTAAGTTGTTG 5' |

**Mitochondrial dynamics studies by confocal microscopy**

Image acquisition of fibroblasts and MEFs was performed in a 0.25% BSA extracellular medium (ECM) consisting of 121 mM NaCl, 5 mM $NaHCO_3$ , 4.7 mM KCl, 1.2 mM $KH_2PO_4$, 1.2 mM $MgSO_4$, 2 mM $CaCl_2$, 10 mM glucose, and 10 mM Na-Hepes, pH 7.4, at 35 °C. Mitochondrial matrix fusion dynamics of ADOA-derived fibroblast was studied at a laser-scanning microscope Nikon Eclipse C2, using a 63X/1.4 ApoPlan objective, located at Advanced Microscopy Facility, Pontificia Universidad Católica de Chile. Time series were performed with excitation with 488 (mt-PAGFP) and 560 (mt-DsRed) nm laser lines, every 5.4s, for a total of 7 minutes. A region of interest (ROI) of 5μm x 5μm was selected to photoactivate PA-GFP with a 405nm laser line. In MEFs, experiments were performed at a laser-scanning microscope system (63×/1.4 NA, LSM 780 NLO with GASP detectors; Carl Zeiss), located at the MitoCare Center, at Thomas Jefferson University. The time series involved excitation 488 (mt-PAGFP) and 560 (mCherry-OMP25) nm laser lines, images were acquired every 1s, to up to 3 minutes. Given the small size of MEFs, ROIs were established as 3μm x 3μm squares; to photoactivate mt-PAGFP by 2 photon laser illumination Chameleon pulsed laser system (760 nm; Coherent). Mitochondrial continuity was determined from the time course of fluorescence inside the ROI normalized to the maximum GFP peak immediately after photoactivation. Diffusion of the photoconverted protein towards neighbor organelles was quantified arbitrarily as the decay 40s post-PA for the patient’s fibroblasts and 20s post-PA for cell lines. Mitochondrial fusion events were quantified as the rapid increase in the GFP fluorescence in acceptor mitochondrion after interaction between a photoactivated mitochondrion and a non-photoactivated mitochondrion; concomitantly, a rapid decrease in mt-PAGFP is observed in the donor

mitochondrion (7). The fusion events frequency was analyzed as previously described, considering events/min= #events/3ROI/min (7).

**Mitochondrial fission frequency**

Mitochondrial fission frequency was quantified as previously reported (8). Briefly, patients' cells transfected with mt-DsRed were imaged in Nikon Eclipse C2, using a 63X/1.4 ApoPlan objective for 7 min. At least three ROIs per cell were selected where individual mitochondria were resolvable and did not leave the focal plane. ROIs were manually scanned frame-by-frame, searching for mitochondrial fission events. The separation of two daughter mitochondria was confirmed when the fluorescence intensity between them was comparable with the background (**SI Appendix Fig. S3C)**. Finally, mitochondrial length was manually determined. Data were plotted as the number of fission events per minute per mitochondrial length. We also measured the number of constrictions per length and the lag time, which is the period between the first constriction observation and the actual mitochondrial division.

**RT-qPCR**

Total RNA was isolated from MEFs using PureLink™ RNA Mini KitTrizol (Invitrogen, CA, USA) according to the manufacturer's instructions. Complementary DNA (cDNA) synthesis was performed using iScript™ cDNA Synthesis Kit (Bio-Rad, CA, USA). Quantitative real-time polymerase chain reactions (qPCR) were performed using a Quant studio 3 using PowerUp™ SYBR™ Green Master Mix according to the manufacturer's recommendations (Applied Biosystems, CA, USA). A list of primers used in this work is given in Table 4. mRNA expression was quantified using the comparative ΔCt method (2-ΔΔCT), using GAPDH as the reference gene. To compare endogenous (mOPA1) vs exogenous (hOPA1) expression, the intra-assay efficiency was determined, and the results were corrected for the efficiency of each primer. The mRNA levels were expressed relative to the mean expression of the control condition.

**Table 4: Primers used to quantify Human *OPA1* exogenous vs Mouse *Opa1* endogenous expression.**

| Mutant | Primers |
|---|---|
| Human *OPA1* | 5' TGCAGAAAGATGACAAAGGCA 3' |

| | |
|---|---|
| | 3' TGGGCAATCATTTCCAACACAC 5' |
| Mouse *Opa1* | 5' ATGTATTCTGAAGTTCTTGATGTTCT 3' |
| | 3' CCAGCACTCTGATCTCCAA 5' |
| Human *GAPDH* | 5' TGCACCACCAACTGCTTAGC 3' |
| | 3' GGCATGGACTGTGGTCATGAG 5' |
| Mouse *GAPDH* | 5' AGGTCGGTGTGAACGGATTTG 3' |
| | 3' TGTAGACCATGTAGTTGAGGTCA 5' |

**Stable cell line generation**

WT and *Opa1*$^{-/-}$ MEFs cells were transfected as described above with a lentiviral plasmid containing the human OPA1 isoform 1, the GTPase mutant *OPA1* c.870+5G>A, the GED mutant *OPA1* c.2713C>T, and a puromycin resistance cassette (pLenti-OPA1). Transfected cells were selected with Puromycin 2µg/mL to obtain a polyclonal stable cell line. The cells were grown in the growth media described above in presence of Puromycin 2µg/mL. The pLenti-OPA1 constructs were obtained from Vector Builder.

**OPA1 Processing**

*Opa1*$^{-/-}$ MEFs expressing *OPA1* GTPase c.870+5G>A or GED .2713C>T mutant were incubated with FCCP 1µM for 1, 3, and 6h. 60 µg of whole cell extract was used for Western blot analysis. OPA1 processing was quantified as the ratio of the OPA1 short form vs OPA1 long form. Import processing was quantified as the ratio of OPA1 total (long + short form) vs OPA1 preprotein.

**OPA1 half-life**

*Opa1*$^{-/-}$ MEFs expressing *OPA1* GTPase or GED mutants were incubated with 50µM of Cycloheximide or 25µM of MG132 for 1, 3, 6h. 60 µg of whole cell extract was used for Western blot analysis.

***In silico* prediction of OPA1 coiled-coil domains**

To predict the possibility of the addition or deletion of coiled-coil domains in OPA1 mutants, a bioinformatic analysis was performed using the online tool DeepCoil

(https://toolkit.tuebingen.mpg.de/tools/deepcoil). *Homo sapiens* OPA1, transcript variant 1 (NM_015560.3) was used as input.

**OPA1 oligomerization analysis**

Whole cell lysate was incubated with the chemical crosslinker Bismaleimidoheaxne (BMH, Thermo Scientific) 200μM for 2h at 4ºC for each condition following the manufacturer's protocol. The reaction was quenched using β-mercaptoethanol. Oligomers were analyzed in a 6% acrylamide SDS-PAGE gel and quantified as the ratio of Monomers/Oligomers.

**OPA1 Immunoprecipitation**

48 hours after transfection, cells were lysed with 300μL Immunoprecipitation (IP) buffer (50mM Tris, 150mM NaCl, 1% Nonidet P-40), supplemented with protease inhibitors and 1mM PMSF. The lysate was centrifugated at 13000g for 20 mins at 4ºC and proteins were quantified by a commercial BCA kit. For immunoprecipitation, 300 μg of proteins were used per condition and supplemented with 30 μL of protein A-Sepharose beads or 30 μL of protein A/G magnetic beads (previously washed 3 times with IP Buffer at 4ºC). 2 μg of unspecific IgG and 300 μL of Ip buffer were added to each tube and incubated for 2h at 4ºC to eliminate unspecific interactions. Next, the beads were separated from the tubes by centrifugation, and the supernatants were incubated with overnight 30 μL of fresh beads and 2 μg of OPA1 antibody. The extract was loaded with 50 μL of loading buffer and denatured for 10 mins at 100ºC.

**OPA1 GTPase activity**

Immunopurified extracts were washed 3 times with IP buffer at 4ºC. The beads were resuspended in a final volume of 78 μL of IP buffer. The final extracts were used for the GTPase activity assay (Malachite Green Phosphate Assay Kit, Sigma) according to manufacturer's instructions. A final concentration of 100 μM GTP was used.

**Image and statistical analysis**

Image analysis was performed using Fiji (ImageJ) software. The statistical analysis was carried out using GraphPad Prism 8 Software. For pairwise comparisons, unpaired Student's

*t*-tests were used for all normally distributed data, whereas Mann-Whitney *U*-tests were used for nonparametric data. For multiple comparisons, One-way ANOVA followed by Dunnett's or Sidak's multiple comparison test was used to determine the significance of normally distributed data, or Two-way ANOVA followed by multiple *t*-test comparison was used to determine significance. For nonparametric multiple comparisons, a Kruskal-Wallis's test followed by Dunn's multiple comparison test was used to determine significance. In all cases, data not indicated as significant should be considered not statistically different.

## Supplementary Figure Legends

**Figure S1. Donor splice site analysis of *OPA1* splicing defects mutants.**

(**A)** *OPA1* disease-related mutations, protein product prediction, and clinical ADOA phenotype, evaluated in this study. [a] Subject's age (years) when the biopsy was taken. [b] Subject's age (years) when subnormal vision and/or optic atrophy was first diagnosed.

(**B**) Western blot densitometry from data shown in Figure1A-B. Data are mean ± SEM of ≥ 4 independent experiments. **P*<0.05, ***P*<0.01, ****P*<0,001 vs Respective control condition.

Blue color is indicative for GTPase mutants and red color for GED mutants.

**(C)** RT-PCR of *OPA1* exon 8 and 27 from control and ADOA-derived patients carrying the splicing defect mutants *OPA1*c.870+5G>A and *OPA1*c.2818+5G>A. Right panel shows the quantification of the intensity of the bands. Each band intensity was quantified and normalized against the respective control amplicon.

**(D)** Exon skipping scheme on splice defect mutants.

**(E)** Location of Acceptor and Donor splice sites in *OPA1* isoform 1 exon 8 and exon 27. Arrows show the intronic mutation for *OPA1* c.870+5G>A and *OPA1* c.2818+5G>A.

**(F)** *In silico* prediction of splice score changes of natural donor splice site for exon 8 mutant *OPA1* c.870+5G>A and exon 27 mutant *OPA1* c.2818+5G>A using the bioinformatic tools HSF and MaxEnt. Both approximations establish a threshold where is predicted the presence of a Donor splice site.

HSF: Human Splice Finder (3). MaxEnt: Maximum Entropy model (4).

**Figure S2. Mitochondrial ultrastructure perturbations in ADOA-derived fibroblasts carrying GTPase and GED mutations.**

(**A-B)** Representative images of mitochondrial shape classification. Scale bar = 500nm. Quantification of shape descriptors. Bar charts show mean ± SEM of same images used in A.

(**C-D)** Ultrastructure mitochondrial cristae shape classification and quantification in ADOA-derived fibroblasts. Scale bar = 100nm.

Data are mean ± SEM of ≥ 3 independent experiments. ***P*<0.01, ****P*<0.001, *****P*<0.0001 vs respective control. Error bars represent SEM.

**Figure S3. ADOA-derived fibroblasts carrying *OPA1* GTPase mutation c.870+5G>A display a beads-on-string phenotype.**

**(A)** Time course of mt-DsRed positive cell showing a mitochondria beads-on-string event**.** White arrows indicate where the intermittent narrowing of long mitochondria leads to a bead-on-string morphology. Scale bar = 10µm.

**(B)** EM microscopy shows mitochondria from different cells with apparent beads-on-string phenotype; arrowheads show narrowing of long organelles. Scale bar = 500nm.

**(C)** Time course of mt-DsRed positive cell showing a mitochondrial fission event. White arrows show the position of a single mitochondrial fission event. Double white arrows show a single mitochondrial constriction that results in a non-productive fission event. Black line shows the fission lag time, defined by the time in which the organelle constriction starts and finishes in a productive fission event. Scale bar = 10µm.

**(D)** Bar graph showing the organelle constriction/µm.

**(E)** Bar graph showing the fission lag time.

Data are mean ± SEM of ≥ 3 independent experiments. ***P*<0.01 vs Control. Error bars represent SEM.

**Figure S4. *OPA1* mutants used in this study**.

**(A)** Table including information on protein mutation, the type of mutation, the domain and subdomain affected, the clinical effect described in the literature, the specific mutation effect, and predicted protein length and molecular weight.

**(B)** OPA1 mutants generated in-vitro using OPA1 WT isoform 1 plasmid as a template. Histograms show Sanger sequencing confirming the mutations in the plasmid.

**Figure S5. Validation of WT and mutant *OPA1* plasmid expression.**

**(A-B)** Western blot and quantification of expression of *OPA1* WT isoform 1 plasmid in *Opa1*$^{-/-}$ MEFs.

**(C-H)** Bar charts showing Western blot quantification from Figure 4A. Data are mean ± SEM of ≥ 3 independent experiments. ***P*<0.01, *****P*<0.0001 vs *Opa1*$^{-/-}$. Error bars represent SEM.

**(I-J)** Western blot and quantification of overexpression of *OPA1* WT isoform 1 in WT MEFs.

**(K-P)** Bar charts showing Western blot quantification from Figure 4B. Data are mean ± SEM of ≥ 3 independent experiments. **P*<0.05, ***P*<0.01, *****P*<0.0001 vs WT. #*P*<0.05, ##*P*<0.01 vs WT + OPA1 WT Error bars represent SEM.

**(Q)** Table showing RT-qPCR of exogenous *OPA1* (ex.*OPA1*) mutants mRNA levels vs endogenous *Opa1* (en.*Opa1*) form in WT MEFs.

**(R)** RT-qPCR of endogenous *Opa1* mRNA levels in WT MEFs upon overexpression of *OPA1* mutants.

**(S-T)** Western blot and quantification of OPA1 and Drp1 upon overexpression of OPA1 mutants in WT MEFs.

**(U)** Representative images of WT MEFs stably overexpressing *OPA1* WT, *OPA1*c.870+5G>A and *OPA1*c.2713C>T

Blue and red bars represent GTPase and GED mutants, respectively.

**Figure S6. Expression of *OPA1* GTPase and GED region-specific mutants have low or zero mitochondrial fusion dynamics activity in *Opa1* $^{-/-}$ background.**

**(A)** Cells acutely co-expressing OMM-targeting mCherry-OMP25, mt-PAGFP, and OPA1 mutants. Each row displays experiments pre and 20s post-photoactivation of 3x3 µm ROIs (white squares) by 2 photon laser illumination (760 nm), acquired upon 488 and 560 nm laser excitation; the right panel shows inset from the middle panel, displaying 1 ROI (white dashed square) highlighting the extent of mt-PAGFP diffusion.

**(B)** Quantification of mitochondrial network morphology of *Opa1*$^{-/-}$ MEFs expressing *OPA1* mutants classified as Elongated, Intermediate, and Fragmented. Data are at least 10 cells per condition from ≥ 3 independent experiments (WT = 23 cells, *Opa1*$^{-/-}$ = 24 cells, *Opa1*$^{-/-}$ +*OPA1*WT = 23 cells, *Opa1*$^{-/-}$ +*OPA1*c.870+5G>A = 20 cells, *Opa1*$^{-/-}$ +*OPA1*c.899G>A = 30 cells, *Opa1*$^{-/-}$ +*OPA1*c.1334G>A = 12 cells, *Opa1*$^{-/-}$ +*OPA1*c.2708delTTAG = 16 cells, *Opa1*$^{-/-}$ +*OPA1*c.2713C>T = 17 cells, *Opa1*$^{-/-}$ +*OPA1*c.2818+5G>A = 10 cells.

**(C)** Quantification of mt-PAGFP decay after photoactivation. Lanes are means of individual ROIs.

**(D)** Bar chart displays the mt-PAGFP fluorescence decay 20s post-PA. Data are mean ± SEM of cells used in B.
**(E)** Mitochondrial fusion events frequency. Bar charts show mean ± SEM of cells used in B.
**(F)** Quantification of mitochondrial fusion duration (time to completion of mt-PAGFP transference from a donor to an acceptor mitochondrion). Bar charts show mean ± SEM of cells used in B.
Data are mean ± SEM. ***$P$<0,001, ****$P$<0.0001 vs *Opa1*$^{-/-}$. ####$P$<0.0001 vs WT.
Blue and red bars represent GTPase and GED mutants, respectively.

**Figure S7. OPA1 mutants and MICOS oligomerization.**
**(A)** Quantification of the time gap between the start of the OMM and IMM fusion as shown in Figure 6A. Bar charts show mean ± SEM.
**(B-C)** OPA1 oligomerization assay in *Opa1*$^{-/-}$ MEFs expressing *OPA1* mutants, by using the chemical crosslinker BHM 200μM and resolved in an SDS-PAGE gel. The bar chart shows the ratio of Oligomers/Monomers. n = 5.
**(D)** *Opa1*$^{-/-}$ MEFs were transfected with *OPA1* WT or the mutants *OPA1* c.889C>T, *OPA1* c.1334G>A, *OPA1* c.2818+5G>A. Oligomers were evaluated using the chemical crosslinker BMH.
(**E-F**) OPA1 oligomerization assay in *WT* MEFs expressing *OPA1* mutants, by using the chemical crosslinker BHM 200μM and resolved in an SDS-PAGE gel. The bar chart shows the ratio of Oligomers/Monomers. n = 5.
**(G)** Mic60 and Mic19 protein levels in *Opa1*$^{-/-}$ MEFs transfected with *OPA1* WT, *OPA1* c.870+5G>A or *OPA1* c.2713C>T. n = 4.
**(H-I)** Mic60 oligomerization assay in *Opa1*$^{-/-}$ MEFs expressing *OPA1* mutants. n = 5.
**(J)** Mic60 and Mic19 protein levels in WT MEFs transfected with *OPA1* WT, *OPA1* c.870+5G>A or *OPA1* c.2713C>T. n = 4.
**(K-L)** Mic60 oligomerization assay in WT MEFs expressing *OPA1* mutants. n = 3.
**(M)** Quantification of OPA1 protein levels from Figure 7D, as a function of time. n = 3.
**(N)** Quantification of OPA1 accumulation kinetic from Figure 7G. n = 3.
**(O)** Representative Western blot of autophagy marker LC3 I/II, GAPDH, and mitochondrial mass marker mtHsp70.
**(P)** Quantification of Western blot data from S7O. n = 4.
Data are mean ± SEM. Error bars indicate SEM.
Blue and red bars represent GTPase and GED mutants, respectively.

**Figure S8. *In-silico* analysis of OPA1 mutants coiled-coils domain prediction**.
**(A)** *OPA1* isoform 1 analysis using bioinformatic tool DeepCoil (9).
**(B)** *OPA1* c.870+5G>A DeepCoil analysis.
**(C)** *OPA1* c.2713C>T DeepCoil Analysis.
**(D)** *OPA1* c.2818+5G>A Deep coil analysis.

**Movie S1. Mitochondria from patient's cells carrying the *OPA1* GTPase c.870+5G>A suffer frequent matrix constrictions exhibiting a beads-on-a-string phenotype**. SkM fibroblasts transfected with mt-DsRed and visualized by confocal microscopy (Nikon Eclipse C2). Images were acquired every 5 s.

**Movie S2. Mitochondrial membrane mixing visualized by high resolution microscopy.** Visualization of mitochondrial fusion and membrane OMM-IMM mixing of two different mitochondria expressing mCherry-OMP25 (OMM) and COXIV8aGFP (IMM) by high-resolution confocal microscopy (Zeiss 880 with Airyscan detector). Video shows a Z-projection of 5 slices in 0.19 μm steps. Images were acquired every 3 s.

**References for SI Information.**


1. L. Young, J. Sung, G. Stacey, J. R. Masters, Detection of Mycoplasma in cell cultures. *Nat Protoc* **5**, 929–34 (2010).
2. G. Csordás, *et al.*, Imaging Interorganelle Contacts and Local Calcium Dynamics at the ER-Mitochondrial Interface. *Mol Cell* **39**, 121–132 (2010).
3. F. O. Desmet, *et al.*, Human Splicing Finder: An online bioinformatics tool to predict splicing signals. *Nucleic Acids Res* (2009) https:/doi.org/10.1093/nar/gkp215.
4. G. Yeo, C. B. Burge, Maximum entropy modeling of short sequence motifs with applications to RNA splicing signals in *Journal of Computational Biology*, (2004) https:/doi.org/10.1089/1066527041410418.
5. A. Olichon, *et al.*, Effects of OPA1 mutations on mitochondrial morphology and apoptosis: Relevance to ADOA pathogenesis. *J Cell Physiol* **211**, 423–430 (2007).
6. V. Eisner, G. Lenaers, G. Hajnóczky, Mitochondrial fusion is frequent in skeletal muscle and supports excitation-contraction coupling. *Journal of Cell Biology* **205**, 179–195 (2014).
7. X. Liu, D. Weaver, O. Shirihai, G. Hajnóczky, Mitochondrial "kiss-and-run": interplay between mitochondrial motility and fusion-fission dynamics. *EMBO J* **28**, 3074–3089 (2009).
8. W.-K. Ji, A. L. Hatch, R. A. Merrill, S. Strack, H. N. Higgs, Actin filaments target the oligomeric maturation of the dynamin GTPase Drp1 to mitochondrial fission sites. *Elife* **4**, 1–25 (2015).
9. L. Zimmermann, *et al.*, A Completely Reimplemented MPI Bioinformatics Toolkit with a New HHpred Server at its Core. *J Mol Biol* **430**, 2237–2243 (2018).

**A**

Figure S1

| Gene Mutation | Protein Mutation | Mutation type | Domain | Gender | Age[a] | Disease onset[b] | Phenotype | ADOA+ phenotype |
|---|---|---|---|---|---|---|---|---|
| c.870+5G>A | p.Lys262_Arg290 Del | Splice defect | GTPase | F | 36 | 8 | ADOA+ | Mild myopathy, muscle cramps, severe migraines |
| c.889C>T | p.Gln297X | Nonsense mutation | GTPase | F | 48 | <5 | ADOA+ | Peripheral neuropathy, prominent spastic paraplegia |
| c.2713C>T | p.Arg905X | Nonsense mutation | GED | F | 60 | 16 | ADOA | – |
| c.2818+5G>A | p.Val903_Lys940 Del_Ins Glu | Splice defect | GED | M | 65 | <5 | ADOA | – |

**B**

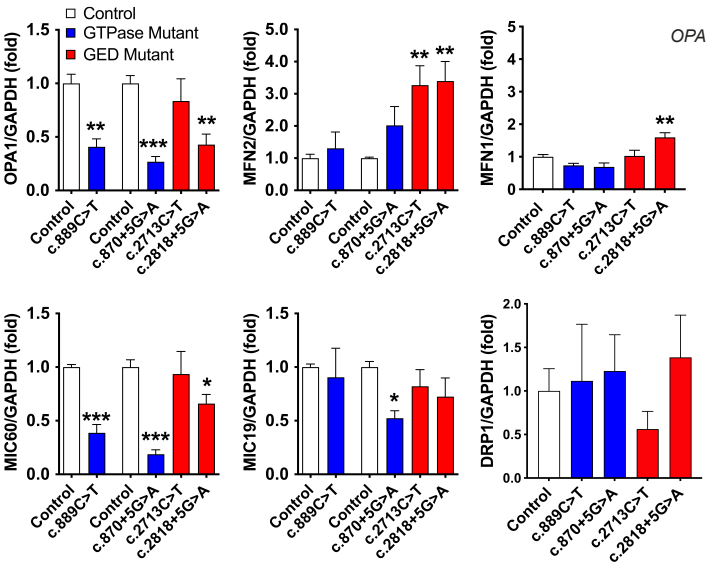


**C**

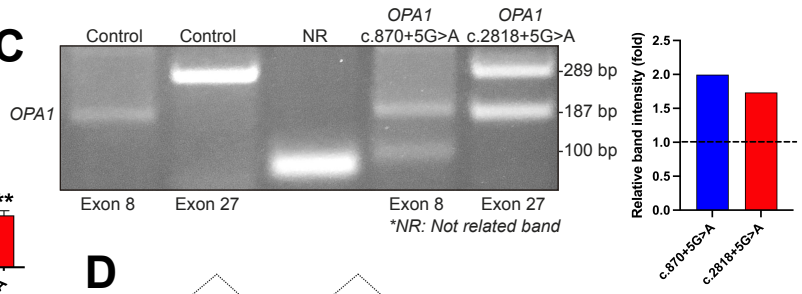


**D**

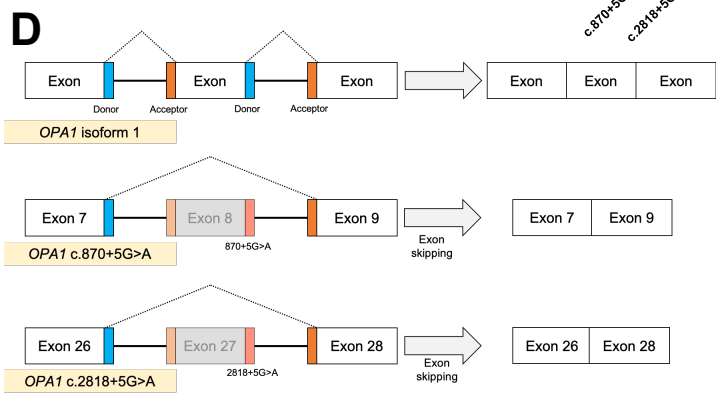


**E**

*OPA1* isoform 1 Exon 8 c.870+5G>A

Acceptor splice site aaatttttacagAAATCTTTGATTGACATGTATTCTGAAGTTCTTGATGTTCTCTCTGATTATGATGCCAGTTATAATACGC
AAGATCATCTGCCACGGgtatgt Donor splice site Donor splice site
5g>a

*OPA1* isoform 1 Exon 27 c.2818+5G>A

Acceptor splice site ttctttaaacagTTAGGCGATTAGAGAAAAATGTTAAAGAGGTATTGGAAGATTTTGCTGAAGATGGTGAGAAGAAGAT
TAAATTGCTTACTGGTAAACGCGTTCAACTGGCGGAAGACCTCAgtgagt
5g>a

**F**

| | Splicing prediction | | |
|---|---|---|---|
| ***OPA1* isoform 1** | **Donor Site** | **HSF Score Threshold >65** | **MaxEnt Score Threshold >3** |
| **Exon 8** | CGGgtatgt | 86.34 | 8.79 |
| **c.870+5g>a** | CGGgtatat | **74.17** | **4.36** |
| **Exon 27** | TCAgtgagt | 81.53 | 7.68 |
| **c.2818+5g>a** | TCAgtgaat | **69.37** | **-2.81** |

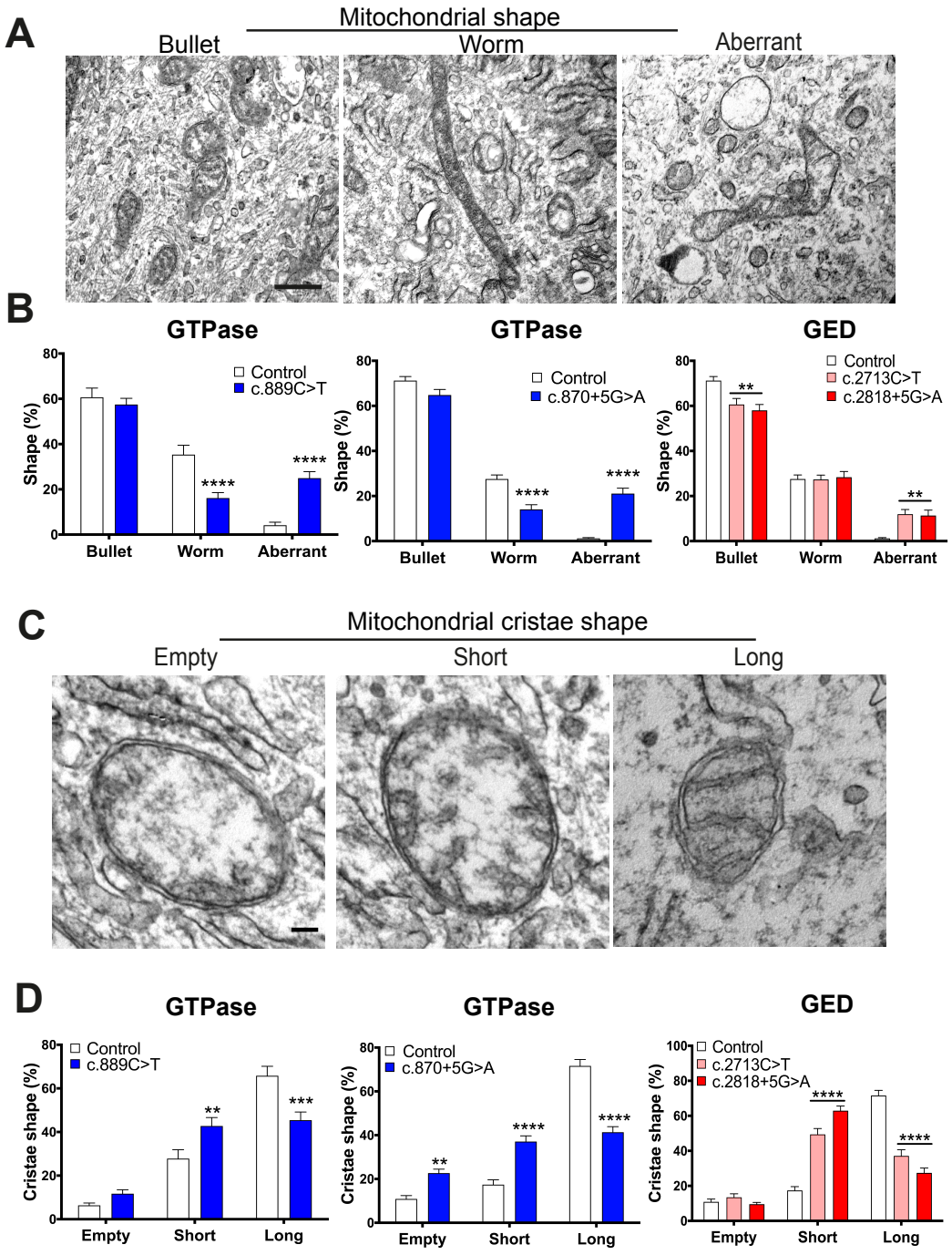
A
Mitochondrial shape
Bullet
Worm
Aberrant
B
GTPase
Control
c.889C>T
Shape (%)
Bullet
Worm
Aberrant
GTPase
Control
c.870+5G>A
GED
Control
c.2713C>T
c.2818+5G>A
C
Mitochondrial cristae shape
Empty
Short
Long
D
GTPase
Cristae shape (%)
GED

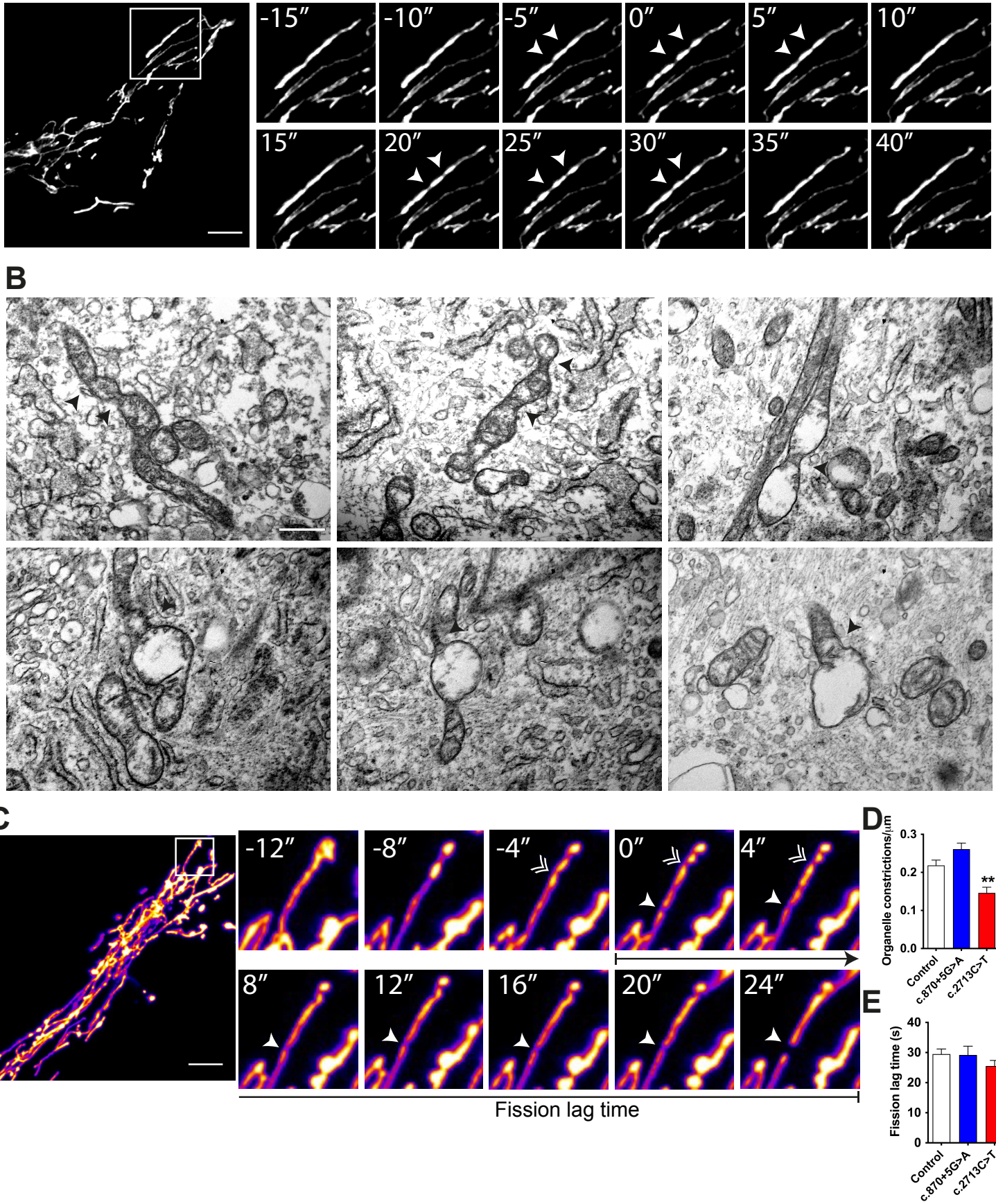
A
-15″
-10″
-5″
0″
5″
10″
15″
20″
25″
30″
35″
40″
B
C
-12″
-8″
-4″
0″
4″
8″
12″
16″
20″
24″
Fission lag time
D
Organelle constrictions/μm
0.3
0.2
0.1
0.0
**
Control
c.870+5G>A
c.2713C>T
E
Fission lag time (s)
40
30
20
10
0
Control
c.870+5G>A
c.2713C>T

**A**

Figure S4

| cDNA mutation | Protein mutation | Mutation type | Specific mutation effect | Domain | Subdomain | Lengh | Predicted MW (kDa) |
|---|---|---|---|---|---|---|---|
| c.870+5G>A | p.Lys262_Arg290 Del | Exon skipping | Loss of 29 aa exon 8 | GTPase | GTPase | 931 aa | 108 |
| c.889C>T | p.Gln297X | Stop codon | Nonsense mutation in GTPase domain | GTPase | G1 motif | 296 aa | 34.6 |
| c.899G>A | p.Gly300Glu | Point mutation | Point mutation GTPase pocket | GTPase | G1 motif | 960 aa | 111 |
| c.1334G>A | p.Arg445His | Point mutation | Point mutation GTPase domain | GTPase | GTPase | 960 aa | 111 |
| c.2708delTTAG | p.Val903GlyfsX3 | Frameshift | Frameshit mutation GED, loss of 55 aa | GED | GED | 904 aa | 105 |
| c.2713C>T | p.Arg905X | Stop codon | Nonsense mutation in GED, loss of 55 aa | GED | GED | 904 aa | 105 |
| c.2818+5G>A | p.Val903_Lys940 Del_Ins Glu | Exon skipping | Loss of 37 aa exon 27 | GED | GED | 923 aa | 107 |

**B**

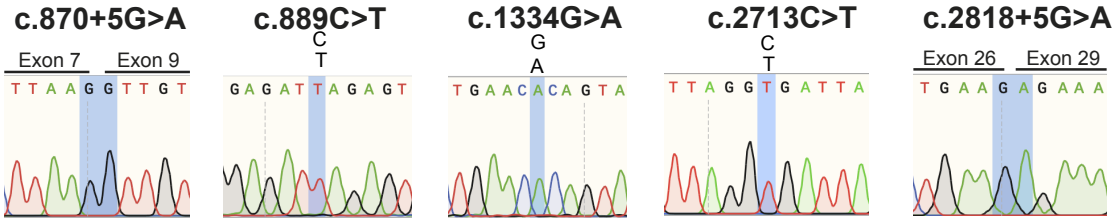

Figure S5

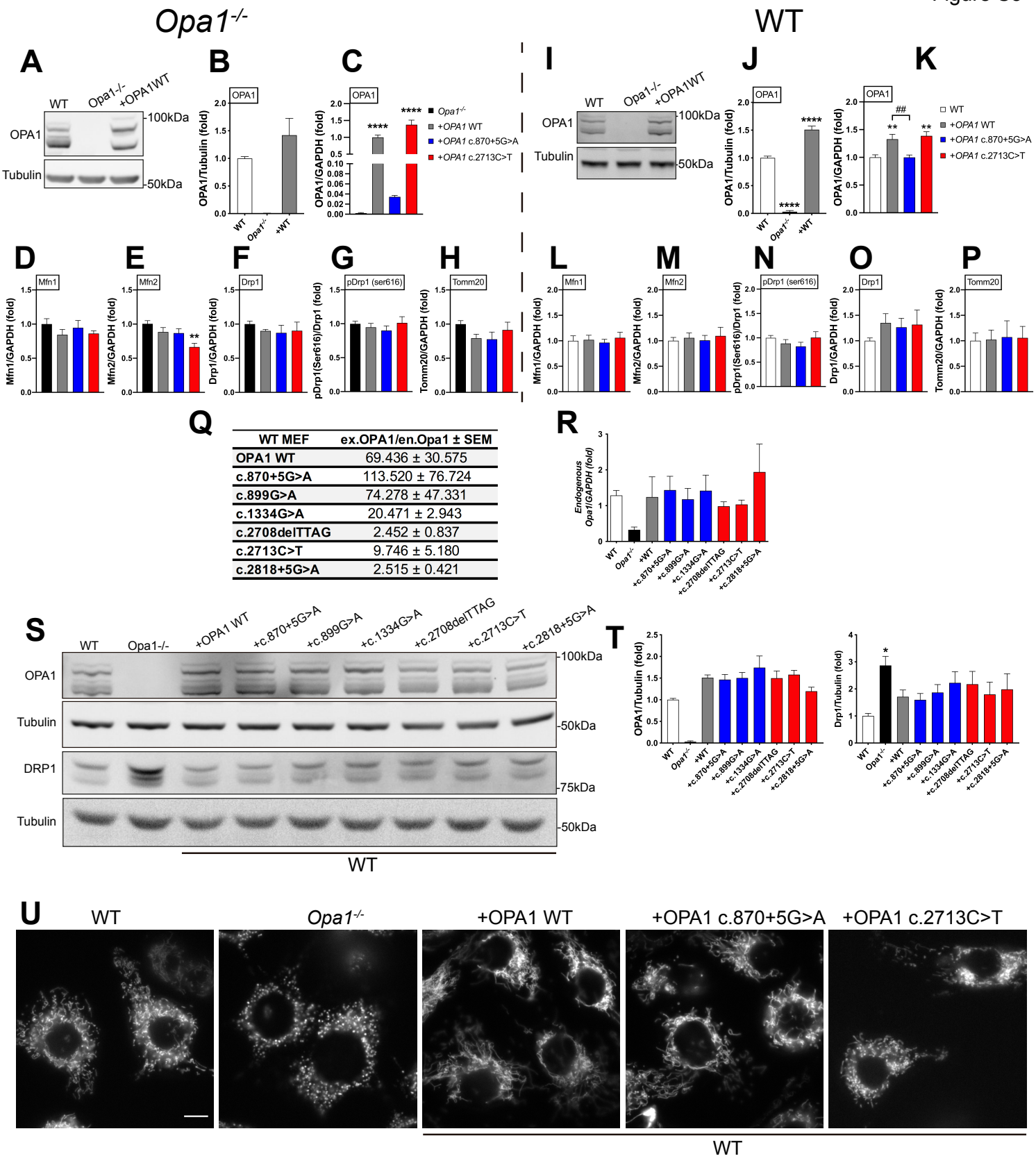


| WT MEF | ex.OPA1/en.Opa1 ± SEM |
|---|---|
| OPA1 WT | 69.436 ± 30.575 |
| c.870+5G>A | 113.520 ± 76.724 |
| c.899G>A | 74.278 ± 47.331 |
| c.1334G>A | 20.471 ± 2.943 |
| c.2708delTTAG | 2.452 ± 0.837 |
| c.2713C>T | 9.746 ± 5.180 |
| c.2818+5G>A | 2.515 ± 0.421 |

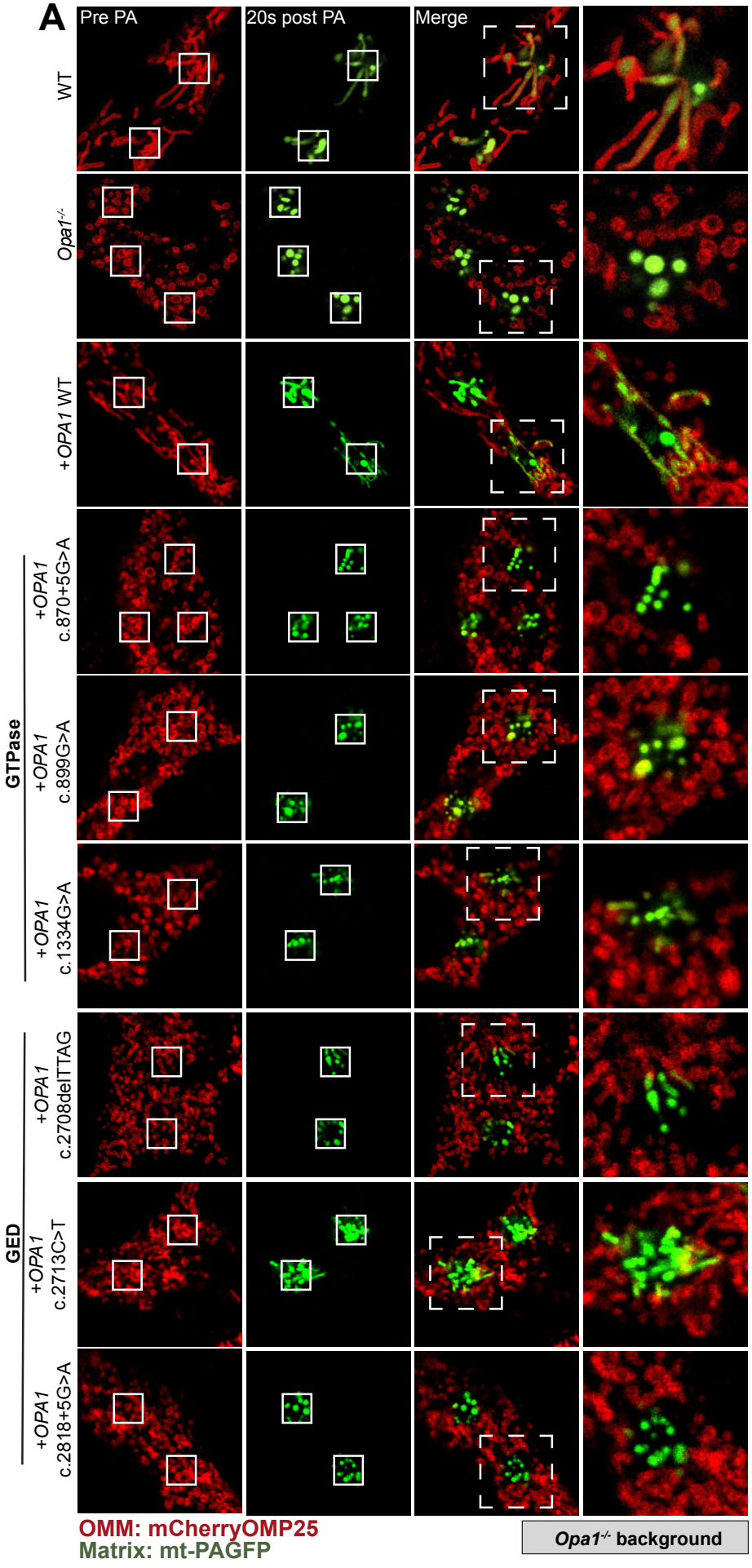
A
Pre PA
20s post PA
Merge
WT
Opa1-/-
+OPA1 WT
+OPA1 c.870+5G>A
+OPA1 c.899G>A
+OPA1 c.1334G>A
+OPA1 c.2708delTTAG
+OPA1 c.2713C>T
+OPA1 c.2818+5G>A
GTPase
GED
OMM: mCherryOMP25
Matrix: mt-PAGFP
Opa1-/- background

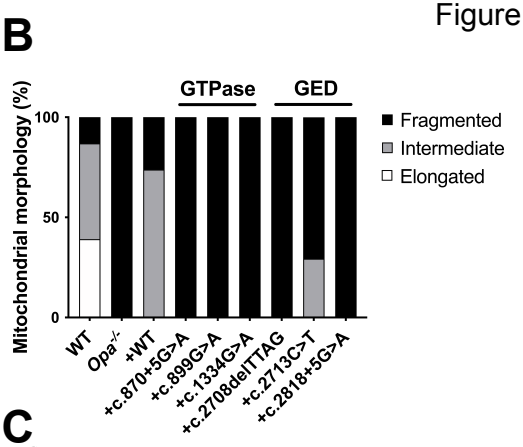
B
GTPase
GED
Mitochondrial morphology (%)
Fragmented
Intermediate
Elongated
WT
Opa1-/-
+WT
+c.870+5G>A
+c.899G>A
+c.1334G>A
+c.2708delTTAG
+c.2713C>T
+c.2818+5G>A

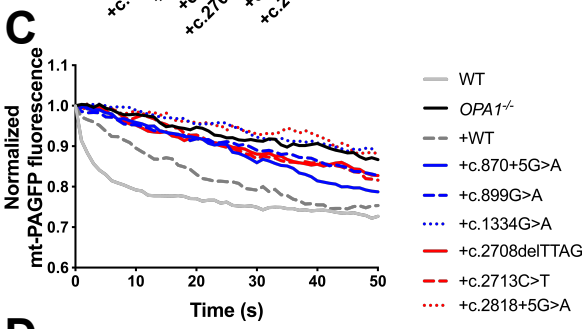
C
Normalized mt-PAGFP fluorescence
Time (s)
WT
OPA1-/-
+WT
+c.870+5G>A
+c.899G>A
+c.1334G>A
+c.2708delTTAG
+c.2713C>T
+c.2818+5G>A

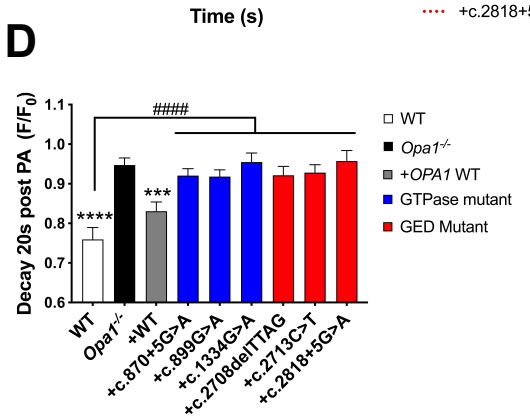
D
Decay 20s post PA (F/F0)
####
****
***
WT
Opa1-/-
+OPA1 WT
GTPase mutant
GED Mutant

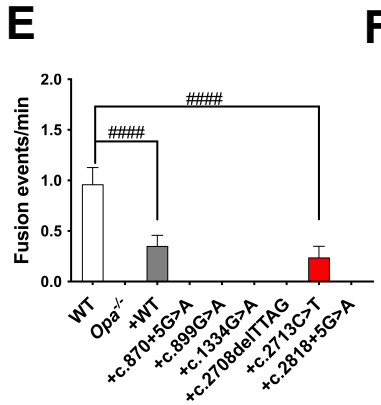
E
Fusion events/min
####
####

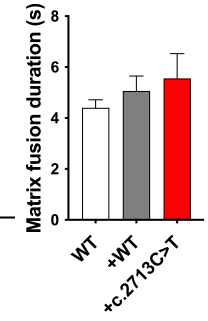
F
Matrix fusion duration (s)

Figure S7

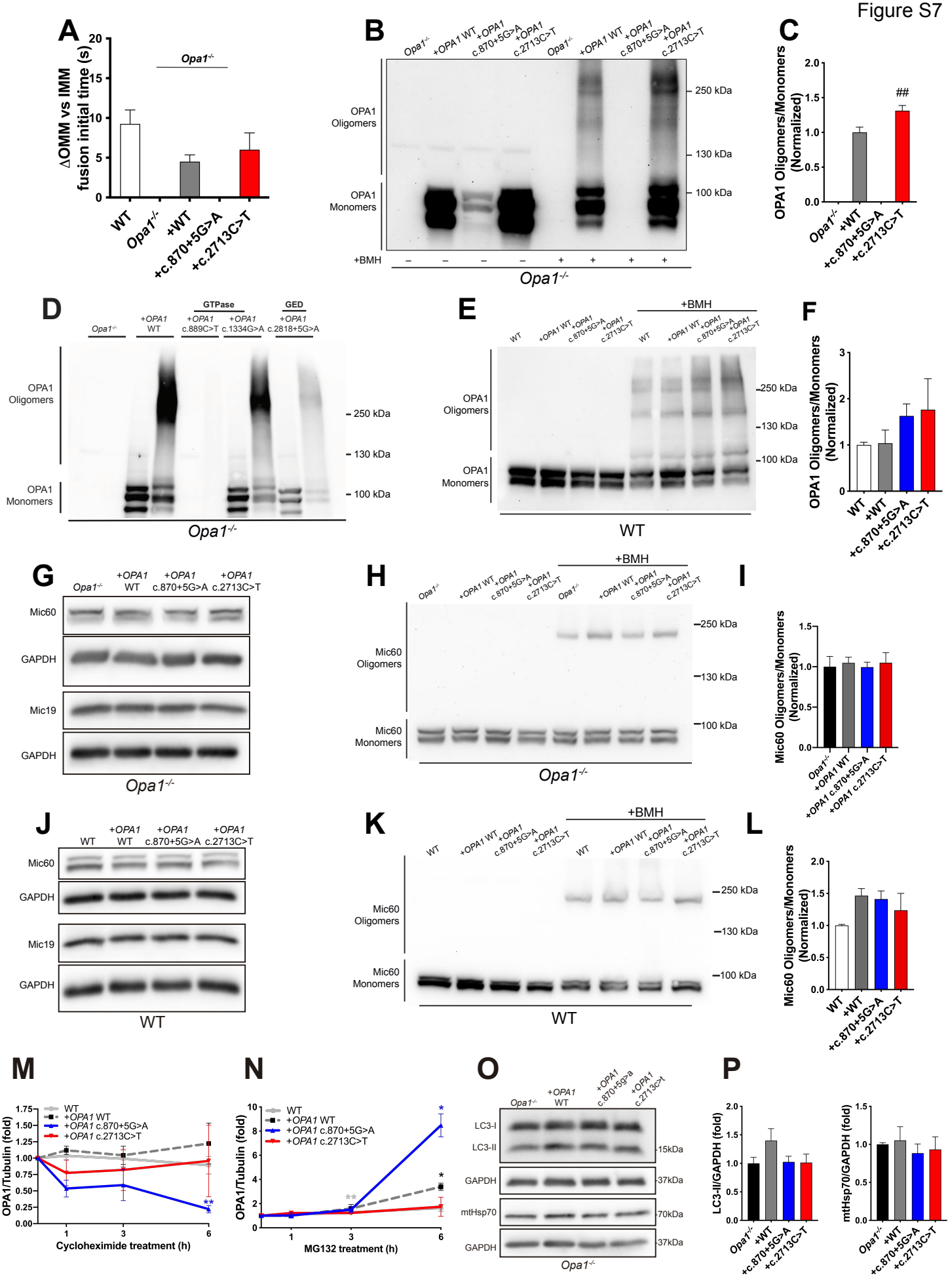
A
ΔOMM vs IMM fusion initial time (s)
Opa1-/-
WT
Opa1-/-
+WT
+c.870+5G>A
+c.2713C>T
B
Opa1-/-
+OPA1 WT
+OPA1 c.870+5G>A
+OPA1 c.2713C>T
OPA1 Oligomers
OPA1 Monomers
250 kDa
130 kDa
100 kDa
+BMH
Opa1-/-
C
OPA1 Oligomers/Monomers (Normalized)
##
D
GTPase
GED
Opa1-/-
+OPA1 WT
+OPA1 c.889C>T
+OPA1 c.1334G>A
+OPA1 c.2818+5G>A
OPA1 Oligomers
OPA1 Monomers
250 kDa
130 kDa
100 kDa
Opa1-/-
E
+BMH
WT
+OPA1 WT
+OPA1 c.870+5G>A
+OPA1 c.2713C>T
OPA1 Oligomers
OPA1 Monomers
250 kDa
130 kDa
100 kDa
WT
F
OPA1 Oligomers/Monomers (Normalized)
G
Opa1-/-
+OPA1 WT
+OPA1 c.870+5G>A
+OPA1 c.2713C>T
Mic60
GAPDH
Mic19
GAPDH
Opa1-/-
H
+BMH
Mic60 Oligomers
Mic60 Monomers
250 kDa
130 kDa
100 kDa
Opa1-/-
I
Mic60 Oligomers/Monomers (Normalized)
Opa1-/-
+OPA1 WT
+OPA1 c.870+5G>A
+OPA1 c.2713C>T
J
WT
+OPA1 WT
+OPA1 c.870+5G>A
+OPA1 c.2713C>T
Mic60
GAPDH
Mic19
GAPDH
WT
K
+BMH
Mic60 Oligomers
Mic60 Monomers
250 kDa
130 kDa
100 kDa
WT
L
Mic60 Oligomers/Monomers (Normalized)
M
OPA1/Tubulin (fold)
WT
+OPA1 WT
+OPA1 c.870+5G>A
+OPA1 c.2713C>T
Cycloheximide treatment (h)
N
OPA1/Tubulin (fold)
WT
+OPA1 WT
+OPA1 c.870+5G>A
+OPA1 c.2713C>T
MG132 treatment (h)
O
Opa1-/-
+OPA1 WT
+OPA1 c.870+5G>a
+OPA1 c.2713C>t
LC3-I
LC3-II
15kDa
GAPDH
37kDa
mtHsp70
70kDa
GAPDH
37kDa
Opa1-/-
P
LC3-II/GAPDH (fold)
mtHsp70/GAPDH (fold)
Opa1-/-
+WT
+c.870+5G>A
+c.2713C>T

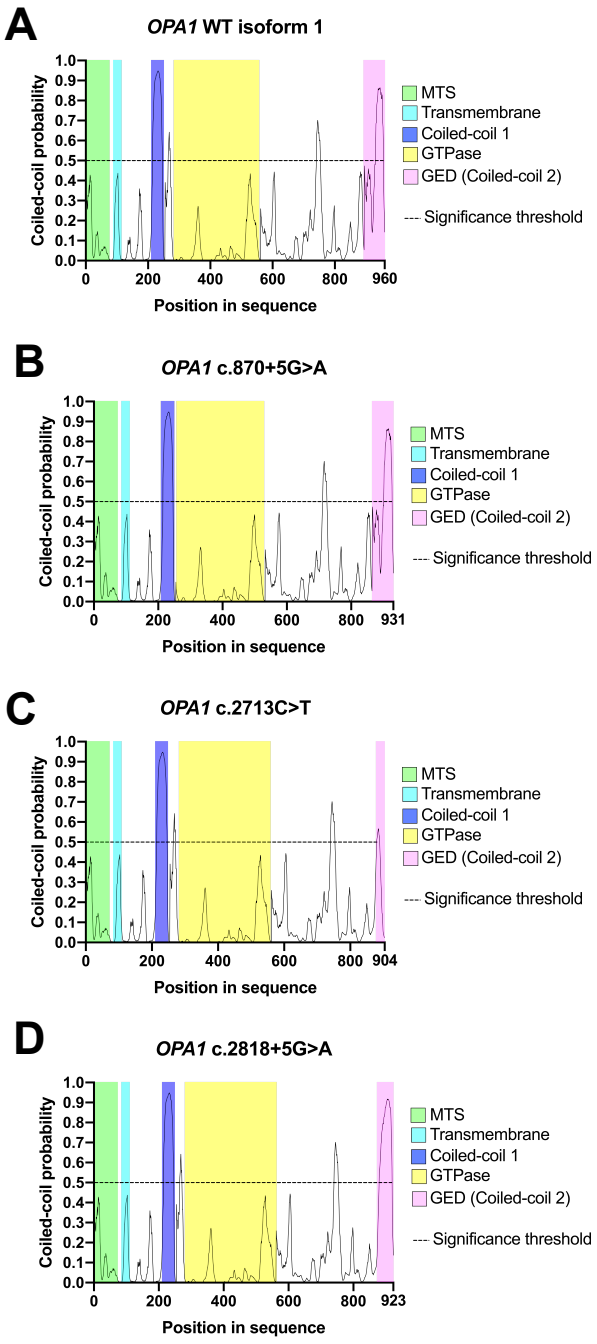
A
OPA1 WT isoform 1
Coiled-coil probability
Position in sequence
MTS
Transmembrane
Coiled-coil 1
GTPase
GED (Coiled-coil 2)
--- Significance threshold
B
OPA1 c.870+5G>A
C
OPA1 c.2713C>T
D
OPA1 c.2818+5G>A